

Regulation of sialic acid transport and catabolism in *Haemophilus influenzae*

Jason W. Johnston,¹ Anthony Zaleski,¹
Simon Allen,² Joe M. Mootz,¹ David Armbruster,^{3,†}
Bradford W. Gibson,² Michael A. Apicella^{1*} and
Robert S. Munson Jr^{3,4}

¹Department of Microbiology, University of Iowa, Iowa City, IA 52242, USA.

²Buck Institute for Age Research, 8001 Redwood Blvd., Novato, CA 94945, USA.

³Center for Microbial Pathogenesis, Columbus Children's Research Institute and ⁴The Ohio State University, Columbus, OH 43205, USA.

Summary

Virulence of nontypeable *Haemophilus influenzae* (NTHi) is dependent on the decoration of lipooligosaccharide with sialic acid. This sugar must be derived from the host, as NTHi cannot synthesize sialic acids. NTHi can also use sialic acid as a carbon source. The genes encoding the sialic acid transporter and the genes encoding the catabolic activities are localized to two divergently transcribed operons, the *siaPT* operon and the *nan* operon respectively. In this study, we identified SiaR as a repressor of sialic acid transport and catabolism in NTHi. Inactivation of *siaR* resulted in the unregulated expression of the genes in both operons. Unregulated catabolism of sialic acid in the *siaR* mutant resulted in the reduction of surface sialylation and an increase in serum sensitivity. In addition to SiaR-mediated repression, CRP, the cAMP receptor protein, was shown to activate expression of the *siaPT* operon but not the *nan* operon. We describe a model in which SiaR and CRP work to modulate intracellular sialic acid levels. Our results demonstrate the importance of SiaR-mediated regulation to balance the requirement of surface sialylation and the toxic accumulation of intracellular sialic acid.

Introduction

Haemophilus influenzae is a common inhabitant of the upper respiratory tract of humans and is a frequent cause

of upper and lower respiratory tract infections. Encapsulated *H. influenzae* strains have the ability to cause invasive diseases including meningitis while unencapsulated nontypeable *H. influenzae* (NTHi) generally cause mucosal infections including otitis media in children and bronchitis in patients with chronic obstructive pulmonary disease. The lipooligosaccharide (LOS) is known to be a major virulence factor of both encapsulated and nontypeable strains.

Sialic acid (5-*N*-acetylneuraminic acid, Neu5Ac) is incorporated into the LOS as a terminal non-reducing sugar. Sialylation of the LOS is believed to contribute to NTHi survival in the host by mimicking human glycosphingolipids (Mandrell *et al.*, 1992) and protecting NTHi against killing mediated by the alternative complement pathway (Hood *et al.*, 1999; 2001; Figueira *et al.*, 2007) although the mechanisms of protection in NTHi are unknown. The addition of sialic acid to the LOS by the sialyltransferase encoded by *lic3A* is phase-variable (Weiser *et al.*, 1990). Organisms isolated from infected chinchillas are predominately *lic3A*-on phase variants and have sialic acid present on their LOS, suggesting that sialylation provides a selective advantage to NTHi *in vivo* (Bouchet *et al.*, 2003). Inactivation of *siaB*, the gene encoding the CMP-Neu5Ac synthetase, results in the inability of the mutant to produce sialic acid-containing glycoforms. These organisms are serum sensitive and completely avirulent in the chinchilla model for otitis media (Bouchet *et al.*, 2003). Sialic acid-containing glycoconjugates are also known to be a major component of NTHi biofilms and are required for biofilm formation in the chinchilla middle ear (Greiner *et al.*, 2004; Jurcisek *et al.*, 2005). NTHi is unable to synthesize sialic acids; therefore, decoration of NTHi glycoconjugates with sialic acid is dependent on exogenous sialic acids. Inactivation of the sialic acid transporter in NTHi prevents incorporation of sialic acid into the NTHi glycoconjugates and also leads to reduced viability of biofilms grown *in vitro* (Allen *et al.*, 2005).

Sialic acid can be used as a carbon source by *H. influenzae* (Fig. 1A) (Vimr *et al.*, 2000; 2004). In *Escherichia coli*, the genes encoding for sialic acid catabolism are found in two separate operons: one that encodes for NanT (the sialic acid transporter), NanA, NanE and NanK while the genes encoding for NagA and NagB are found elsewhere on the chromosome (Plumbridge and Vimr, 1999; Ringenberg *et al.*, 2003; Vimr

Accepted 19 July, 2007. *For correspondence. E-mail michael-apicella@uiowa.edu; Tel. (+1) 319 335 7807; Fax (+1) 319 335 9006. †Present address: Department of Biochemistry and Molecular Biology, Medical School of South Carolina, Charleston, SC 29425, USA.

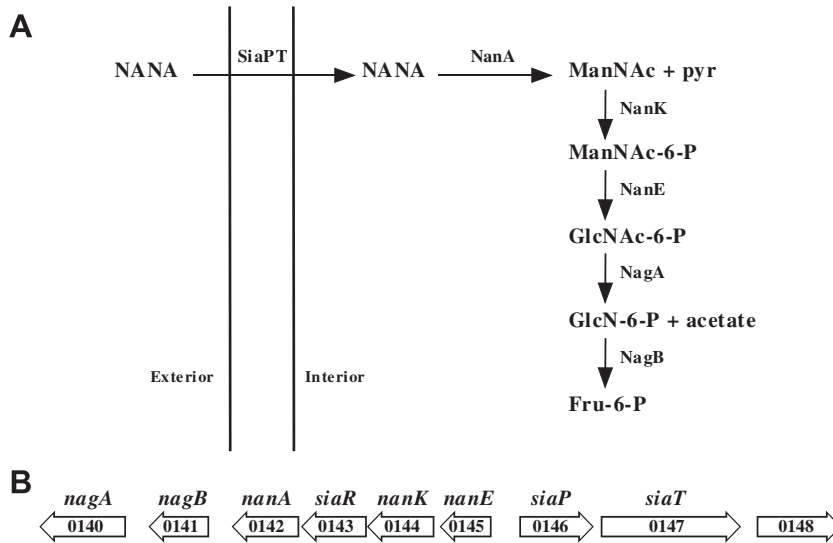


Fig. 1. A. Sialic acid transport and metabolism pathway of *H. influenzae*. Sialic acid is transported by the SiaPT transporter. The genes of the *nan* operon encode for the enzymes that convert Neu5Ac into fructose-6-phosphate, which can then enter glycolysis.

B. Organization of sialic acid transport and metabolism genes in *H. influenzae*. The gene number corresponds to the HI number based on the *H. influenzae* KW-20 Rd genome annotation.

et al., 2004). In NTHi, sialic acid is transported into the cell by a tripartite ATP-independent periplasmic (TRAP) transporter that is encoded by *siaPT* (Allen *et al.*, 2005; Severi *et al.*, 2005). In contrast to the gene arrangement in *E. coli*, the enzymes required for the complete conversion of sialic acid to fructose-6-phosphate are encoded by the genes of a single operon (Fig. 1B). The *siaPT* and the *nan* operons of NTHi are adjacent to each other and divergently transcribed (Vimr *et al.*, 2000; 2004). The *nan* operon also contains a gene that encodes for a putative transcriptional regulator, HI0143 (Vimr *et al.*, 2000). It has previously been speculated that the protein encoded by HI0143 may function to regulate the expression of the sialic acid metabolism and transport operons (Vimr *et al.*, 2004) although no work has been published to support this hypothesis.

We examined the role of HI0143 in regulation of the Neu5Ac catabolic pathway. This transcriptional regulator, which we have designated SiaR, was found to repress the operons that encode the sialic acid transporter and the genes involved in sialic acid catabolism. Expression of the transporter, but not the catabolic pathway, was induced by cAMP via CRP in the absence of SiaR. Inactivation of *siaR* increased sensitivity to human serum. This demonstrates the necessity of stringent control of *nan* operon expression for protection of the organism from complement-mediated killing.

Results

Construction of a mutant deficient in the putative transcriptional regulator SiaR and identification of genes regulated by SiaR

HI0143 was identified as a potential transcriptional regulator due to its homology to RpiR family transcriptional

regulators. Members of the RpiR family are characterized by the presence of both a helix–turn–helix DNA-binding domain and a sugar isomerase (SIS) domain (Bateman, 1999). The SIS domain is found in a wide variety of proteins and functions to bind a phosphosugar molecule (Bateman, 1999). In *E. coli*, RpiR represses *rpiB* which encodes for a ribose phosphate isomerase (Sorensen and Hove-Jensen, 1996). Other members of this family have not been characterized. HI0143 differs significantly from NanR, the sialic acid-dependent transcriptional regulator found in *E. coli*, a member of the FadR/GntR family of transcriptional regulators (Kalivoda *et al.*, 2003). Based on the protein sequence HI0143 and NanR are not homologous (15% similarity). As HI0143 is located in the operon that encodes for the enzymes involved in Neu5Ac catabolism (Fig. 1B), it seems likely that HI0143 regulates sialic acid catabolism.

To determine the role of HI0143, which we have named *siaR*, in the regulation of sialic acid catabolism we constructed a *siaR* mutant. The mutant was constructed by replacing the *siaR* gene with a promoterless kanamycin resistance cassette. Microarray analysis was used to investigate the role of SiaR in the regulation of gene expression. Changes in gene expression were examined using competitive hybridizations between labelled cDNA prepared from RNA samples isolated from early to mid-logarithmic phase cultures of wild-type 2019 and 2019*siaR* grown in sRPMI-based medium containing 100 μ M Neu5Ac. Microarray comparisons were performed with three independent pairs of RNA preparations. Each pair of RNA preparations was hybridized to two slides. The expression profile for the 2019*siaR* mutant revealed that the expression of three putative operons was increased in the absence of SiaR: HI0145–HI0140, HI0146–HI0149 and HI1537–HI1540 (Table 1). Using reverse transcription

Table 1. Transcriptional analysis of 2019*siaR* mutant.

Gene ID	Gene	Function	Expression ratio (2019 <i>siaR</i> /2019)	
			Microarray analysis	Real-time RT-PCR
HI0140	<i>nagA</i>	<i>N</i> -acetylglucosamine-6-phosphate deacetylase	4.9	ND
HI0141	<i>nagB</i>	Glucosamine-6-phosphate isomerase	11.9	ND
HI0142	<i>nanA</i>	<i>N</i> -acetylneuraminate lyase	14.3	ND
HI0144	<i>nanK</i>	<i>N</i> -acetylmannosamine kinase	7.2	ND
HI0145	<i>nanE</i>	<i>N</i> -acetylmannosamine-6-phosphate 2-epimerase	10.4	20.9 ± 2.7
HI0146	<i>siaP</i>	Sialic acid transporter, periplasmic solute receptor	15.8	14.3 ± 1.7
HI0147	<i>siaT</i>	Sialic acid transporter, integral membrane component	12.3	ND
HI0148		Conserved hypothetical protein	6.8	ND
HI0148.1		Hypothetical protein	7.9	ND
HI0149		Hypothetical protein	2.3	ND
HI1537	<i>licA</i>	Choline kinase	11.2	14.7 ± 3.6
HI1538	<i>licB</i>	Choline transporter	3.8	ND
HI1539	<i>licC</i>	CTP-phosphorylcholine cytidyltransferase	6.5	ND
HI1540	<i>licD</i>	NDP-choline transferase	4.4	ND

polymerase chain reaction (RT-PCR) it was determined that HI0145–HI0140 and HI0146–HI0149 form two separate operons (data not shown). These operons encode for the proteins involved in Neu5Ac catabolism and transport. The HI1537–HI1540 gene cluster encodes for enzymes involved in the transport and addition of phosphorylcholine (ChoP) to the LOS. Expression of the genes of the three operons ranged from a 2.3-fold increase for HI0149 to a 15.8-fold increase for HI0146 (Table 1). Quantitative RT-PCR (qRT-PCR) performed on the same three pairs of RNA samples used for the microarray studies was used to confirm the results of the microarray analysis using primer and probe sets for HI0145 (*nanE*), HI0146 (*siaP*) and HI1537 (*licA*), which encode for the first gene of each putative operon. The results of qRT-PCR analysis were in good concordance with the microarray data (Table 1). Further analysis demonstrated that the apparent regulation of the *lic1* gene cluster was due to phase variation rather than SiaR-mediated regulation as detailed in the *Supplementary material*.

Complementation of the *siaR* mutation by the introduction of a single copy of *siaR* ectopically into the genome was able to partially restore the repression of *nanE* and *siaP* as observed by qRT-PCR. Analyses were performed from cultures grown in the same conditions used in the microarray analysis. The complemented *siaR* mutant had a 5.2 ± 0.2 -fold and 3.9 ± 0.5 -fold reduction in the expression of *nanE* and *siaP* when compared with the 2019*siaR* mutant strain. These data indicate that SiaR is responsible for the regulation of the *nanE*- and *siaP*-containing operons.

SiaR binds to the nanE-siaP intergenic region

The transcriptional analysis indicated that both the *nan* and *siaPT* operons were upregulated in the *siaR* mutant. As the operons are divergently transcribed from a

common intergenic region, it appears that SiaR regulates the expression of both operons from a single intergenic site. An electrophoretic mobility shift assay (EMSA) was used to demonstrate the interaction of SiaR with this intergenic region. SiaR was expressed with a C-terminal His-tag fusion using the pET-24 protein expression plasmid. Probes for the entire intergenic region between *nanE* and *siaP*, the region upstream of *licA* and the P2 porin promoter were generated by PCR. The P2 porin gene is believed to be constitutively expressed in NTHi and thus this promoter region was used as a negative control (Munson and Tolan, 1989). The binding of purified SiaR to these DNA probes was examined using EMSA (Fig. 2A). SiaR was found to bind only to the *nanE-siaP* promoter region and not to either the *licA* or P2 promoters, demonstrating that the interaction of SiaR with DNA is site-specific. The inability of SiaR to bind to the *licA* promoter further supports our finding that SiaR does not regulate the expression of the *lic1* operon. A preliminary analysis using additional DNA fragments that span the *nan* and *siaPT* operons did not reveal the presence of any additional SiaR binding sites.

It has previously been demonstrated that the NanR regulator of *E. coli* is displaced from its operator by the addition of Neu5Ac (Kalivoda *et al.*, 2003). The ability of SiaR to bind to the *nanE-siaP* intergenic region was examined in the presence of a 1000-fold excess (1 mM) of Neu5Ac, *N*-acetylmannosamine, *N*-acetylglucosamine and *N*-acetylglucosamine-6-phosphate (Fig. 2B). In the presence of the sugars tested, SiaR was still able to bind to the DNA probe. This suggests that either these sugars are unable to induce expression of SiaR-regulated genes or derepression occurs by an alternative mechanism.

DNase I footprinting was used to further map the location of the SiaR binding site in the *nanE-siaP* intergenic region. SiaR was found to protect a 53 bp region located 113 bp from the start codon of *nanE* and 185 bp from the start

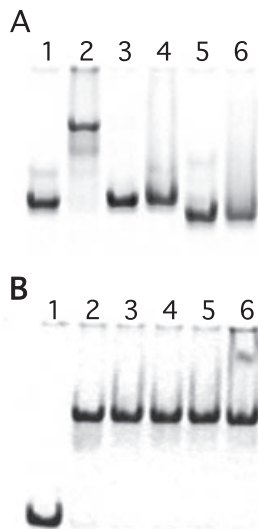


Fig. 2. Electrophoretic shift mobility assay.

A. Binding of SiaR to the *nanE-siaP* promoter region (lanes 1 and 2), *lic1* promoter region (lanes 3 and 4) and the P2 promoter (lanes 5 and 6). Probes were run in the absence (lanes 1, 3 and 5) and presence (lanes 2, 4 and 6) of purified SiaR.

B. Binding of SiaR to the *nanE-siaP* promoter region in the presence of various sugars. Lane 1, unbound probe; lane 2, SiaR without sugar; lane 3, SiaR with Neu5Ac; lane 4, SiaR with *N*-acetylmannosamine; lane 5, SiaR with *N*-acetylglucosamine; and lane 6, SiaR with *N*-acetylglucosamine-6-phosphate.

codon of *siaP* (Fig. 3). The protected region overlapped the predicted CRP binding site by three bases (Fig. 4). The close proximity of the SiaR and CRP binding sites suggests the possibility that the regulators may interact to modulate the expression of the two adjacent operons.

Neu5Ac-dependent derepression of *nanE* and *siaP* expression *in vivo*

The role of Neu5Ac-mediated derepression was examined *in vivo*. In strain 2019, we observed no significant change in the expression of either *nanE* or *siaP* when cells were grown in the presence or absence of 100 μ M Neu5Ac as determined by qRT-PCR (-1.3 ± 0.1 -fold

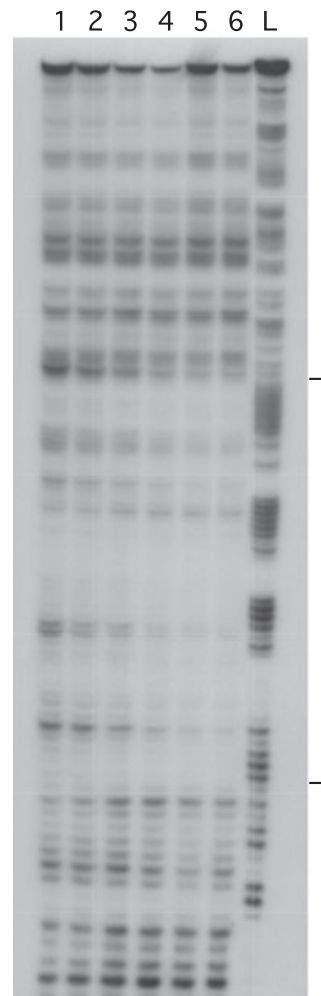


Fig. 3. DNA footprint analysis of the *nanE-siaP* intergenic region. Lane 1, probe without SiaR, lanes 2–6, probe with increasing concentrations of SiaR (0.15–2.5 μ M), lane L, a G+A ladder used as a marker. The bracket denotes the region protected by SiaR.

and -1.5 ± 0.1 -fold respectively). The addition of cAMP along with Neu5Ac also failed to induce expression (data not shown). In order to prevent catabolism of sialic acid, regulation of expression was examined in a

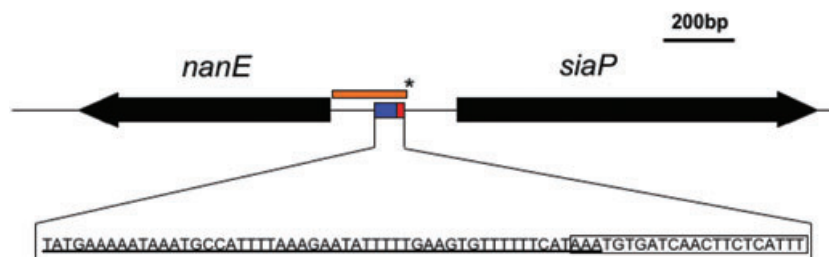


Fig. 4. The *nanE-siaP* intergenic region. A schematic representation of the 350 bp intergenic region indicating the relative location of the SiaR (blue) and CRP (red) binding sites. The probe used for DNase I footprinting is indicated as an orange box with the asterisk designating the labelled end. The underlined sequence indicates the region protected by SiaR. The boxed sequence corresponds to the predicted CRP binding site.

2019*nanA* mutant strain. There was little change in the expression of both *nanE* and *siaP* mRNA levels when 2019*nanA* was grown in the presence or absence of 100 μ M Neu5Ac (1.4 ± 0.2 -fold and 1.1 ± 0.2 -fold respectively). The possibility that intracellular Neu5Ac did not accumulate to significant levels, even in the *nanA* mutant background, was explored by creating a *nanAsiaB* double mutant. This mutant can neither catabolize Neu5Ac nor activate Neu5Ac to CMP-Neu5Ac. When the expression of *nanE* and *siaP* was measured in the absence and presence of 100 μ M Neu5Ac in the double mutant, Neu5Ac-mediated induction was observed. Expression of *nanE* was 14 ± 0.4 -fold higher in the presence of Neu5Ac while *siaP* was induced 3.3 ± 0.2 -fold. These data indicate that under the conditions tested, the conversion of Neu5Ac into CMP-Neu5Ac prevented the induction of both the *nan* and *siaPT* operons in the 2019*nanA* mutant.

CRP activates expression of *siaPT* but not *nanE*

Genes from the *nan* and *siaPT* operons have been identified as potential CRP-regulated genes by microarray analysis of the competence regulon of *H. influenzae* Rd (Redfield *et al.*, 2005). To examine the role of CRP in the regulation of sialic acid transport and metabolism, *crp* was inactivated in the 2019*siaR* mutant strain, resulting in a 2019*siaRcrp* double mutant. Expression of *nanE* and *siaP* in 2019*siaRcrp* was compared with the expression of these genes in 2019*siaR* using qRT-PCR. Expression of *nanE* did not vary significantly between strains 2019*siaR* and 2019*siaRcrp* (1.6 ± 0.1 -fold higher in 2019*siaR*) when cells were grown in sRPMI-based medium. In contrast, expression of *siaP* was upregulated 14 ± 0.1 -fold in 2019*siaR* compared with 2019*siaRcrp*, demonstrating the CRP dependence of the *siaP* promoter. When the growth medium was supplemented with 1 mM cAMP, *siaP* expression was upregulated 35 ± 0.1 -fold in 2019*siaR* compared with 2019*siaRcrp*, demonstrating a further increase in *siaP* promoter activity. We conclude that expression of the sialic acid transporter genes, *siaPT*, are positively regulated by cAMP and CRP while expression of the *nan* operon is cAMP/CRP independent.

Serum sensitivity of the *siaR* mutant

The possibility that the increased catabolism of sialic acid in the *siaR* mutant could have adverse effects on protection from complement-mediated killing was investigated. Sialylation of LOS protects the bacterium from complement-mediated killing by normal human serum (Hood *et al.*, 1999). Conversely, unregulated catabolism of sialic acid might result in a sialic acid-deficient LOS,

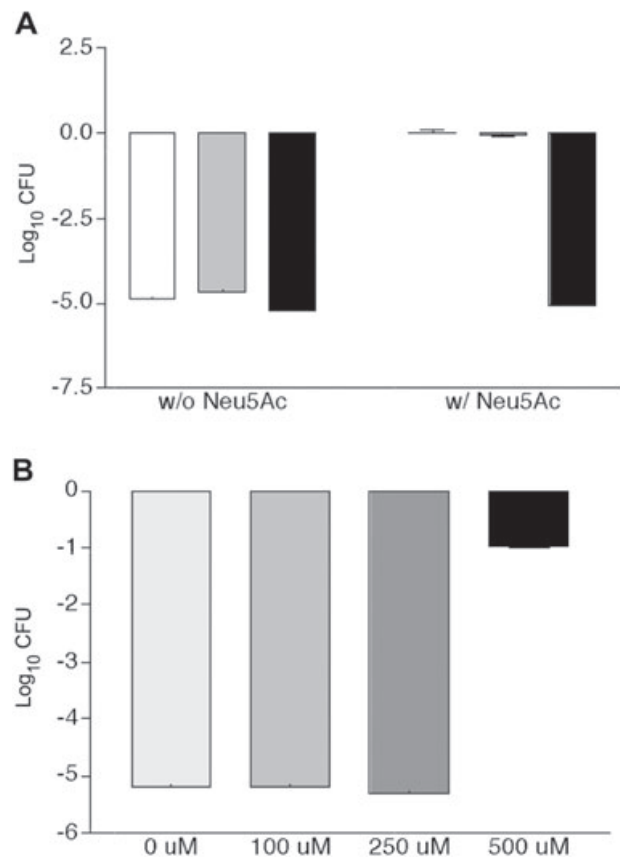


Fig. 5. Resistance to serum killing.

A. Strains 2019 (open bars), 2019*licA* (JWJ070; grey bars) and 2019*siaRlicA* (JWJ071; black bars) were grown to mid-log phase in sBHI broth with and without 100 μ M Neu5Ac. Bacteria were exposed to normal human serum for 30 min at 37°C and plated to obtain viable cell counts. Results are expressed as log₁₀ change in cfu between treated and untreated bacteria.

B. 2019*siaRlicA* was grown in various concentrations of Neu5Ac prior to the assay.

which would render the organism serum-sensitive. The presence of ChoP on the LOS increases sensitivity to serum killing by activation of the classical pathway via the C-reactive protein (Weiser *et al.*, 1998). Thus, in order to examine the serum sensitivity of the *siaR* mutant without complications due to variations of ChoP levels, a *licA* mutant background was used for this series of experiments. Strains 2019*licA* and 2019*siaRlicA* were both serum-sensitive when grown in medium lacking Neu5Ac (Fig. 5A), consistent with our previously published results (Allen *et al.*, 2005). In contrast, when grown with 100 μ M Neu5Ac, 2019*licA* was serum-resistant while 2019*siaRlicA* remained serum-sensitive (Fig. 5A). As expected, strains incubated with heat-inactivated serum were not killed, demonstrating the complement-dependence of the reaction (data not shown). To further demonstrate that increased catabolism of sialic acid in the *siaR* mutant was responsible for serum sensitivity,

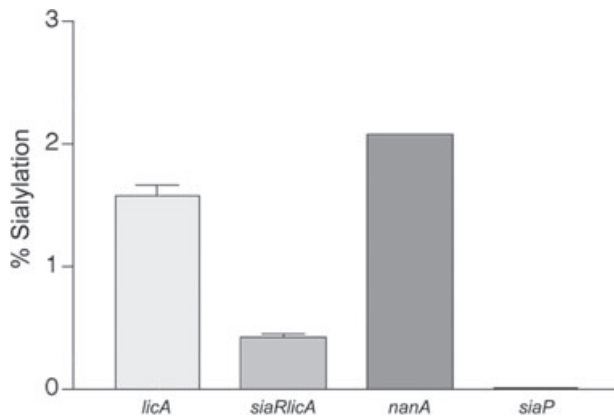


Fig. 6. Sialic acid content of LOS. Sialic acid was released from purified LOS by neuraminidase treatment and quantified using the thiobarbituric acid method. Results are expressed in per cent of sialic acid, by weight. Data from three separate experiments were included in the analysis. *2019licA* and *2019siaRlicA* were found to be significantly different ($P = 0.0035$) using a two-tailed paired *t*-test analysis.

2019siaRlicA was grown in the presence of increasing amounts of Neu5Ac prior to the assay. When grown with 0, 100 and 250 μM Neu5Ac, *2019siaRlicA* was completely sensitive to serum killing (Fig. 5B). Partial protection was observed when *2019siaRlicA* was grown in 500 μM Neu5Ac (Fig. 5B), demonstrating that when cells were grown in extremely high levels of sialic acid, the effects of the inactivation of *siaR* can be overcome. These results indicate that unregulated expression of the sialic acid catabolic pathway results in a serum-sensitive phenotype.

Impact of *siaR* mutation on sialylation of the LOS

It is likely that the observed serum-sensitive phenotype of the *siaR* mutant was due to decreased sialylation of the LOS. In order to demonstrate that there was less sialic acid in the LOS purified from the *siaR* mutant, LOS was purified from broth cultures of *2019licA* and *2019siaRlicA* grown in brain–heart infusion supplemented with 10 $\mu\text{g ml}^{-1}$ haemin and 10 $\mu\text{g ml}^{-1}$ β -NAD (sBHI) containing 100 μM Neu5Ac to replicate the growth conditions used in the serum-killing assay. LOS from strains *2019nanA* and *2019siaP* were used as positive and negative controls respectively. Sialylation of purified LOS was examined using the thiobarbituric acid (TBA) colorimetric assay for sialic acid and by mass spectrometry. Sialic acid was released from the purified LOS by overnight digestion with neuraminidase. The TBA assay was then used to quantify the levels of sialic acid in each digest, comparing to a standard curve. Results were expressed as the percent sialic acid of the LOS, by weight. *2019licA* LOS had 3.8-fold higher sialic acid levels compared with LOS from *2019siaRlicA* (Fig. 6). As expected, LOS from

2019nanA had increased levels of sialic acid while *2019siaP* LOS did not contain detectable sialic acid.

To confirm the TBA colorimetric assay results, LOS isolated from the various mutants was O-deacylated and the resulting O-deacylated LOS (O-LOS) analysed by negative-ion matrix-assisted laser desorption ionization-linear ion trap-mass spectrometry (MALDI-LIT-MS). The O-LOS from various mutants show typical profiles for strain 2019, with B-glycoforms (lactose branch) dominating the spectra (Fig. 7, Table S1). O-LOS isolated from the *2019nanA* mutant is ‘hypersialylated’ with the disialylated B-glycoforms being the most abundant. Of note, the disialylated glycoforms appear to undergo a water loss (-18 , resultant ions marked X in spectra) during mass spectrometry; this loss is not apparent in the monosialylated glycoforms. There are no sialylated glycoforms observed in the O-LOS isolated from *2019siaP* (Fig. 7B), as would be expected for a Neu5Ac transporter mutant. The O-LOS of the *2019licA* mutant (Fig. 7C) shows what could be considered a ‘normal’ degree of sialylation, as there is no defect in any of the genes involved in sialic acid catabolism and transport. As can be seen, the degree of sialylation is less than that of the *2019nanA* mutant (compare Fig. 7A and C). Finally, the O-LOS from the *2019siaRlicA* mutant (Fig. 7D) shows a degree of sialylation that is lower than that observed in the LOS from the *2019licA* mutant (compare Fig. 7C and D). These data correlate well with the TBA assay data and indicate that in the absence of SiaR regulation, incorporation of Neu5Ac into the LOS is reduced. As it is known that sialic acid-containing LOS is required for serum resistance it is likely that the observed increase in serum sensitivity is due to the decreased levels of sialic acid in the LOS of the *siaR* mutant.

Inhibition of growth by Neu5Ac

In *E. coli*, growth of a *nanA* mutant is inhibited by the presence of Neu5Ac in the growth medium (Vimr and Troy, 1985), demonstrating that the accumulation of intracellular sialic acid is toxic to these bacteria. Previous and current work with a *2019nanA* mutant has demonstrated that Neu5Ac minimally affects the growth of *2019nanA*. We found, however, that a *nanAsiaR* double mutant was unable to grow in medium supplemented with Neu5Ac (Fig. 8). The toxicity of Neu5Ac is not dependent on the activation of Neu5Ac to CMP-Neu5Ac as growth of a *2019siaBsiaRnanA* triple mutant was also inhibited by Neu5Ac (data not shown). There are two possibilities for the requirement of the inactivation of *siaR* to observe this growth defect. First, as the toxic effects appear to be due to accumulation of Neu5Ac and not CMP-Neu5Ac, the presence of SiaB may play a role maintaining Neu5Ac levels at a permissive concentration in the wild-type and

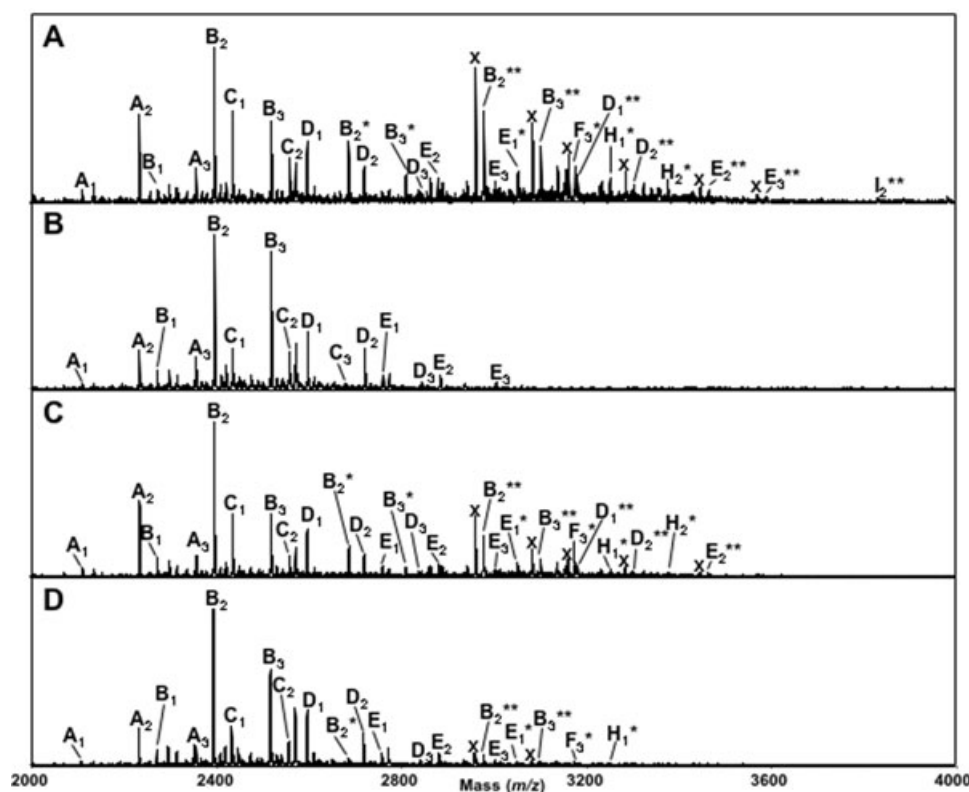


Fig. 7. Negative-ion vMALDI-LIT mass spectra of O-deacylated LOS from (A) 2019*nanA*, (B) 2019*siaP*, (C) 2019*licA* and (D) 2019*siaRlicA* grown in sBHI broth supplemented with 100 μ M Neu5Ac. See Table S1 for molecular weights and proposed compositions. Capital letters designate glycoforms that are acceptors for Neu5Ac. Asterisks indicate addition and number of sialic acid residues; subscript indicates the number of PEA moieties; X indicates ions generated by the loss of water from the adjacent disialylated LOS glycoform.

2019*nanA* strains. Another possibility is that even with an overabundance of intracellular Neu5Ac, SiaR is still able to at least partially repress expression of the transporter. The ability of a *siaBnanA* double mutant to grow in the presence of Neu5Ac (Fig. 8) supports this scenario. Thus, the severe growth defect is only seen when the *siaPT*

operon is completely derepressed. It is likely that both mechanisms contribute to the maintenance of intracellular sialic acid levels.

Discussion

The regulation of surface antigens is an important aspect of virulence. This is especially true when a pathogen can exist as a member of the normal flora. NTHi are found as normal flora in humans and can cause diseases ranging from lower respiratory tract infections to otitis media. The presence of sialic acid on the LOS and biofilm matrix is important for the evasion of the host immune response by NTHi.

Decoration of the LOS with sialic acid is believed to aid the bacteria by mimicking human oligosaccharides (Mandrell *et al.*, 1992) and protecting against complement-mediated killing (Hood *et al.*, 1999; Figueira *et al.*, 2007). Inactivation of *siaB*, the CMP-acetylneuraminic acid synthetase, prevents the addition of Neu5Ac to the LOS and attenuates virulence of the mutant in a chinchilla model of otitis media (Hood *et al.*, 1999; Jurcisek *et al.*, 2005). Depletion of complement in chinchillas that have been infected with a *siaB* mutant allows for the establishment of acute otitis media, demonstrating that the main role of

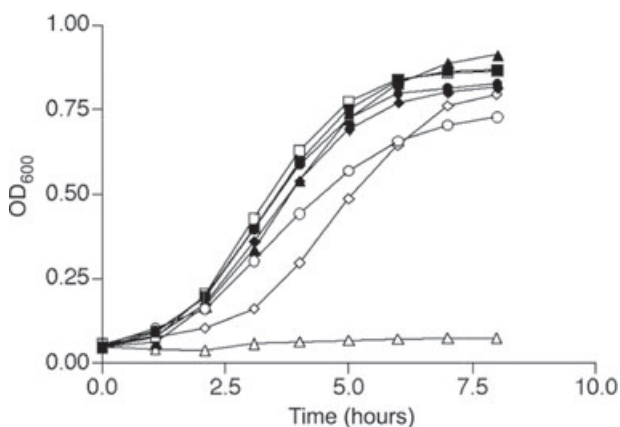


Fig. 8. Growth of 2019 (squares), 2019*nanA* (circles), 2019*siaRnanA* (JWJ037; triangles) and 2019*siaBnanA* (JWJ069; diamonds) in supplemented RPMI broth with (open symbols) and without (closed symbols) 100 μ M Neu5Ac.

sialylation is protection against complement-mediated killing (Figueira *et al.*, 2007). Neu5Ac is also the terminal sugar of the NTHi biofilm matrix component (Greiner *et al.*, 2004) and is required for biofilm formation in the otitis media model (Jurcisek *et al.*, 2005). Biofilm formation *in vitro* also requires sialic acid-containing glycoconjugates as a mutant deficient in the ability to transport, and therefore incorporate, sialic acid into its glycoconjugates fails to produce a normal biofilm (Allen *et al.*, 2005).

The genes required for the uptake and catabolism of Neu5Ac are located together on the chromosome in two divergently transcribed operons (Fig. 1B). The genes *siaP* and *siaT* encode the components of a tripartite ATP-independent periplasmic (TRAP) transporter specific for Neu5Ac (Allen *et al.*, 2005; Severi *et al.*, 2005). The adjacent *nan* operon encodes for the enzymes required for the conversion of Neu5Ac to fructose-6-phosphate, funnelling Neu5Ac into glycolysis (Fig. 1A) (Vimr *et al.*, 2000). Inactivation of *nanA*, which is required for the first step in the catabolic pathway, actually increases fitness in an intranasal infant rat infection model, presumably due to hypersialylation of the LOS (Vimr *et al.*, 2000). This observation indicates that the catabolism of sialic acid is not required for survival within a non-human host and that other carbon and energy sources are available.

SiaR, a transcriptional regulator that has homology to RpiR, has been identified as a repressor of the genes encoding for the transport and catabolism of Neu5Ac. The gene encoding *siaR* is found within the *nan* operon, immediately upstream of *nanA* (Fig. 1B). Inactivation of *siaR* led to increased expression of both the *nan* and *siaPT* operons, supporting its role as a transcriptional repressor. Additionally, purified SiaR bound to an operator that was located in the intergenic region between *nanE* and *siaP*, demonstrating that SiaR directly regulates these two operons rather than acting as part of a cascade. Sialic acid-mediated derepression was not observed in the wild-type or 2019*nanA* mutant strains, presumably because of the rapid activation of intracellular sialic acid by SiaB, the CMP-Neu5Ac synthetase. *In vivo* derepression of *nanE* was observed in a 2019*nanAsiaB* double mutant, supporting this hypothesis.

The presence of a CRP binding site in the intergenic region between *nanE* and *siaP* suggested that CRP could be involved in the activation of one or both of these operons. Studies with a *siaRcrp* double mutant revealed that only the expression of the transporter is activated by CRP and cAMP. This result contradicts a study by Redfield *et al.* (2005) that identified many genes in the *nan* operon as CRP-regulated genes in *H. influenzae* KW-20 Rd. We do not currently understand the basis for the discrepancy.

Based on our results with NTHi strain 2019, we propose the following model. Under normal growth conditions, sialic acid is transported by SiaPT and activated by the

siaB gene product such that sialic acid can be incorporated into LOS and other sialic acid-containing glycoconjugates. When the cells are starved but sialic acid is present in the growth medium, cAMP levels increase and cAMP-CRP activates the expression of the transporter. Sialic acid is imported via SiaPT resulting in the derepression of both the *siaPT* and *nan* operons. The sialic acid is then available for either catabolism or activation by SiaB and subsequent sialylation of the LOS or biofilm matrix. The presence of *siaR* within the *nan* operon will result in an increase in the levels of SiaR when the operon is induced. This autoregulatory mechanism ensures that expression of sialic acid metabolism is kept under constant control.

The protective functions of sialylation and the toxic effects of sialic acid accumulation must be balanced to ensure the survival of NTHi. SiaR is the major factor in preventing both the accumulation of toxic levels of sialic acid and the unrestrained catabolism of sialic acid that would reduce its availability for sialylation. Even in a *siaB-nanA* double mutant, in which sialic acid can accumulate and derepress, SiaR appears to be able to maintain some control over the expression of *siaPT* and prevent the build-up of toxic levels of Neu5Ac. This is evidenced by the ability of the *siaBnanA* mutant to grow in the presence of sialic acid while the *siaBsiaRnanA* triple mutant cannot. In the triple mutant, sialic acid accumulates to levels that inhibit growth. We have also demonstrated that changes in the available sialic acid can have a profound effect on the resistance to complement-mediated killing. The unregulated expression of sialic acid transport and catabolism observed in the *siaR* mutant leads to changes in surface sialylation and confers sensitivity to serum killing. The findings of this study clearly demonstrate the importance of SiaR-mediated control of sialic acid transport and catabolism and surface sialylation and its impact on protection from complement-mediated killing.

Despite the parallel functions of the Neu5Ac-dependent regulators in *E. coli* and *H. influenzae*, we have chosen to distinguish the *Haemophilus* repressor by designating it SiaR. SiaR-mediated regulation of the *nan* operon differs significantly from NanR-mediated regulation in *E. coli*. It was previously shown that Neu5Ac-induced derepression of *nanA* is significantly higher in *E. coli* (200-fold) than *H. influenzae* (twofold) (Vimr *et al.*, 2000). Our data support this finding. Expression of the *nan* operon is not significantly altered in the presence of sialic acid in the wild-type 2019 strain. To observe a significant Neu5Ac-induced change under the conditions we employed, both *nanA* and *siaB* need to be inactivated. There are several reasons for this difference. The turnover of intercellular Neu5Ac by NanA and SiaB may be sufficient in wild-type 2019 to minimize derepression. This may also explain the difference between *H. influenzae* and *E. coli nanA*

Table 2. Strains and plasmids.

Strain or plasmid	Genotype, relevant phenotype or selection marker	Source or reference
Strains		
<i>E. coli</i> DH5 α	F ⁻ ϕ dlacZ Δ M15 Δ (lacZYA-argF) U169 <i>recA1 endA1 hsdR17</i> (r _k ⁻ m _k ⁺) <i>phoA supE44 λ-thi-1 gyrA96 relA1</i>	Invitrogen
<i>E. coli</i> BL21 Star		Invitrogen
NTHi 2019	Clinical respiratory isolate	Campagnari <i>et al.</i> (1987)
NTHi 2019 <i>nanA</i>	NTHi 2019 <i>nanA</i> mutant, kanamycin resistant	
NTHi 2019 <i>siaB</i>	NTHi 2019 <i>siaB</i> mutant, spectinomycin resistant	
JWJ022	NTHi 2019 <i>siaR</i> mutant, kanamycin resistant	This study
JWJ037	NTHi 2019 <i>siaRnanA</i> mutant, kanamycin resistant	This study
JWJ050	NTHi 2019 <i>crp</i> mutant, spectinomycin resistant	This study
JWJ052	NTHi 2019 <i>siaRcrp</i> mutant, kanamycin and spectinomycin resistant	This study
JWJ069	NTHi 2019 <i>siaBnanA</i> mutant, kanamycin and spectinomycin resistant	This study
JWJ070	NTHi 2019 <i>licA</i> mutant, chloramphenicol resistant	This study
JWJ071	NTHi 2019 <i>siaRlicA</i> mutant, kanamycin and chloramphenicol resistant	This study
JWJ074	NTHi 2019 <i>siaBsiaRnanA</i> mutant, kanamycin and spectinomycin resistant	This study
JWJ075	NTHi 2019 <i>siaR</i> complemented mutant, kanamycin and spectinomycin resistant	This study
Plasmids		
pGEM-T Easy	PCR-cloning vector	Promega
pGEM-T	PCR-cloning vector	Promega
pCR2.1-TOPO	PCR-cloning vector	Invitrogen
pET-24(+)	Expression vector	Novagen
pUC19	General cloning vector	New England Biolabs
pUC18K3	Kanamycin resistance cassette	Menard <i>et al.</i> (1993)
pUC19K3	Kanamycin resistance cassette	This study
pSPECR	Spectinomycin resistance cassette	Whitby <i>et al.</i> (1998)
pUC19nanAr_Kn	<i>nanA</i> knockout vector	Greiner <i>et al.</i> (2004)
pCR601.1	HI0601.1 region in pCR2.1	This study
p601.1-Sp2	Ectopic complementation vector	This study
pJJ150	<i>siaR</i> knockout vector	This study
pJJ169	<i>siaRnanA</i> knockout vector	This study
pJJ175	<i>crp</i> region	This study
pJJ181	<i>crp</i> knockout vector	This study
pJJ185	C-terminal his tag SiaR expression vector	This study
pJJ237	<i>cat</i> reporter vector	This study
pJJ245	<i>licA</i> knockout/ <i>cat</i> reporter vector	This study
pJJ256	<i>siaR</i> complementation vector	This study

mutants in their sensitivity to Neu5Ac. It also appears that NanR in *E. coli* is more responsive to Neu5Ac than SiaR as indicated by higher levels of *nan* operon induction in *E. coli* as compared with induction in NTHi. This may be due to fundamental differences between these two repressors. There is very little sequence similarity between NanR and SiaR even though they both are shown to relieve repression *in vivo* in the presence of Neu5Ac. Additionally, SiaR remained bound to the operator even in the presence of Neu5Ac, unlike NanR, indicating that the mechanism of induction may be different between these two systems. This may also be a result of a difference in the relative affinity for Neu5Ac and requires further investigation. Also, the possibility of a co-repressor that works to antagonize derepression may exist.

The differences between NanR and SiaR highlight the relative importance of sialic acid to the respective bacterial species. Sialylation of the LOS is a critical requirement for the survival of most, if not all, NTHi strains. We have demonstrated that slight changes in sialylation can greatly impact the susceptibility of NTHi 2019 to serum killing. The *E. coli* strains that have been studied to date

have the ability to synthesize sialic acid (Vimr *et al.*, 1995). As *H. influenzae* strains lack a biosynthetic pathway for sialic acid biosynthesis, they must scavenge sialic acid from their environment. The relatively low levels of free sialic acid available within the host necessitate that the bacterium efficiently controls sialic acid catabolism in order to sialylate the LOS and other glycoconjugates.

Experimental procedures

Bacterial strains, media and growth

The strains used in this study are listed in Table 2. *E. coli* was grown at 37°C in Luria–Bertani (LB) medium with or without agar (1.5%) and supplemented with antibiotics as needed. NTHi strain 2019 (Campagnari *et al.*, 1987) and derivatives thereof were used in this study. *H. influenzae* was grown at 37°C in the presence of 5% CO₂ on sBHI agar (Difco Laboratories, Detroit, MI). Kanamycin-resistant *H. influenzae* were selected on sBHI agar containing 15 μ g ml⁻¹ ribostamycin in the absence of additional CO₂. Chloramphenicol and spectinomycin were added to sBHI at concentrations of 2 μ g ml⁻¹ and 25 μ g ml⁻¹ respectively. RPMI 1640 medium

(Invitrogen, Carlsbad, CA) was used as a sialic acid-free chemically defined medium. Supplemented RPMI (sRPMI) was prepared with protoporphyrin IX ($1 \mu\text{g ml}^{-1}$), hypoxanthine (0.1 mg ml^{-1}), uracil (0.1 mg ml^{-1}), β -NAD ($10 \mu\text{g ml}^{-1}$) and sodium pyruvate (0.8 mM). Neu5Ac ($100 \mu\text{M}$) was added as indicated.

Construction of mutants

Genetic manipulations were performed using established techniques. Restriction enzymes, Antarctic Phosphatase and T4 polymerase were obtained from New England Biolabs (Beverly, MA) and were used following established protocols. The Expand High Fidelity PCR System (Roche Applied Science, Indianapolis, IN) was used for PCR reactions. Oligonucleotide primers were designed and ordered from Integrated DNA Technologies (Coralville, IA). Plasmids were transformed and maintained in MAX Efficiency DH5 α Chemically Competent cells (Invitrogen). Competent *H. influenzae* cells were prepared using the M-IV method and transformed as described previously (Herriott *et al.*, 1970).

A *siaR* (HI0143) mutant was constructed in NTHi strain 2019 to study the role of SiaR in the regulation of sialic acid transport and metabolism. Regions upstream and downstream of *siaR* were amplified by PCR using primers listed in Table S2 and cloned into pGEM-T Easy (Promega, Madison, WI). Primers were designed to add restriction sites to both ends of the inserts to allow for subcloning. These fragments were then sequentially subcloned into pUC18K3 (Menard *et al.*, 1993) and arranged around the kanamycin resistance cassette, *aphA3*, resulting in pJJ150. The *aphA-3* gene of pUC18K3 lacks both a promoter and transcriptional terminator and should allow for the expression of downstream genes of an operon to be controlled by the native promoter. pJJ150 was linearized and transformed into NTHi 2019, creating strain JWJ022. The correct integration of the cassette and inactivation of *siaR* was confirmed by PCR (results not shown).

To study the role of CRP in the expression of the *nan* and *siaPT* operons, *crp* and *siaRcrp* mutants were constructed. A region spanning *crp* was amplified by PCR and cloned into pGEM-T Easy, resulting in pJJ175. Restriction enzymes BseRI and BmgBI were used to excise a 400 bp fragment from within the gene and replace it with the spectinomycin resistance cassette from pSPECR (Whitby *et al.*, 1998), creating pJJ181. pJJ181 was linearized with EcoRI and transformed into strains 2019 and JWJ022 to create strains JWJ050 and JWJ052 respectively. The correct integration of the cassette was confirmed by PCR (results not shown).

A *siaRnanA* double mutant was constructed. Fragments amplified with primers for regions upstream of *siaR* and downstream of *nanA* were subcloned into pUC19K3. pUC19K3 is a derivative of pUC18K3 with the *aphA-3* cassette in the opposite orientation relative to the *lacZ* promoter. The resulting construct, pJJ169, was used to replace both *siaR* and *nanA* with *aphA-3*. pJJ169 was linearized with EcoRI and HindIII and transformed into NTHi 2019, resulting in strain JWJ037. The correct integration of the cassette was confirmed by PCR (results not shown).

2019*siaB* was transformed with linearized plasmids pUC19_nanAr_Kn (Greiner *et al.*, 2004) and pJJ169 to

create 2019*siaBnanA* (JWJ069) and 2019*siaBsiaRnanA* (JWJ043) double and triple mutants respectively. Correct integration of respective cassettes and confirmation of the *siaB* mutation were confirmed by PCR.

Complementation of the *siaR* mutant

The open reading frame (ORF) HI0601.1 contains an authentic frameshift in the KW-20 genome. We used this region to insert a copy of *siaR* to complement the 2019*siaR* mutant. PCR was used to amplify a 2342 bp fragment from NTHi 2019 genomic DNA using primers 601.1-1 and 601.1-2. This fragment was cloned into pCR2.1-TOPO (Invitrogen) and sequenced. Sequencing confirmed that HI0601.1 was present in NTHi 2019 and that it also contained a frameshift that resulted in a severe truncation of the ORF. This plasmid was designated pCR601.1.

PCR was used to amplify a 1061 bp fragment containing the spectinomycin cassette and its upstream promoter, but not the downstream transcription terminator, from pSPECR using primers SprupBsrGI and SprdnMCS. The product was cloned into pCR2.1-TOPO, and sequenced. The sequence confirmed that the expected DNA fragment had been cloned. This plasmid was designated pCRSp2. The 1108 bp EcoRI (blunt ended)/BsrGI fragment from pCRSp2 was ligated into pCR601.1 which had been digested with BsgI (blunt ended)/BsrGI. This plasmid was designated p601.1-Sp2. The construct was verified by sequencing.

PCR was used to amplify a fragment containing *siaR*. The PCR fragment was cloned into pGEM-T (Promega) and subsequently subcloned into p601.1-Sp2 using SmaI sites. The resulting construct, pJJ256 (Fig. S1), was linearized and transformed into the *siaR* mutant, JWJ022. Correct integration of the construct was confirmed by PCR.

RNA extraction and transcriptional analysis

RNA was extracted using the hot acid phenol method as described previously (Peterson *et al.*, 2000). DNA was removed from extracted RNA by digestion with DNase I (New England Biolabs) and cleaned up with the RNeasy Mini Kit (Qiagen, Valencia, CA). RNA quality was assessed with an Agilent 2100 Bioanalyser (Agilent, Santa Clara, CA) and concentration was determined using a NanoDrop ND-1000 Spectrophotometer (NanoDrop Technologies, Wilmington, DE). For real-time RT-PCR analysis, primer/probe sets were obtained using the Custom TaqMan Gene Expression Service (Applied Biosystems, Foster City, CA). Primer/probe sets were designed using the sequence of HI0145, HI0146 and HI1537 from *H. influenzae* 2019. A primer/probe set for the 16S rRNA of *H. influenzae* was designed and used as a control. The TaqMan One-Step RT-PCR Master Mix Reagents (Applied Biosystems) were used following the manufacturer's protocol. Reactions were set up in triplicate using 20 ng of RNA. Reactions were carried out using an ABI Prism 7700 Sequence Detector (Perkin Elmer, Wellesley, MA) with ABI Prism 7700 v1.7 analysis software. Results were calculated using the comparative C_T method to determine the relative expression ratio between RNA samples. The primer and probe set for HI16S rRNA was used as the

endogenous reference to normalize the results. Data are expressed as mean \pm SD.

Microarray analysis

The DNA microarray and relevant protocols used in this study were described previously (Harrison *et al.*, 2007). The array was prepared from commercial oligonucleotide probes based on the *H. influenzae* KW20 Rd genome (Operon Biotechnologies, Huntsville, AL). cDNA was synthesized and labelled using an indirect labelling method similar to that described in Hegde *et al.* (2000). Two replicate slides were performed for each biological replicate, and three biological replicates were performed per experiment, resulting in 24 data points per gene. Dye intensity normalization was applied by performing LOWESS (subgrid) algorithm to all significant features including exogenous spike bacterial controls. Analysis of variance and replicate averaging was performed using the NIA/NIH ANOVA tool. A False Discovery Rate (FDR) > 0.05 was used to exclude false positives, where $FDR = P^*N/\text{rank}$, P is P -value, N is total number of genes and rank is the gene ordered in increasing P -value. Absent spots, empty spots and positive control spots were excluded from the ANOVA analysis.

Expression and purification of SiaR

SiaR was expressed and purified for further study. Primers were used to amplify *siaR* with the restriction sites HindIII and XhoI on the 5' and 3' ends, respectively. The 70 bases immediately upstream of *siaR* were included to ensure that the native bacterial translation signals were present. The downstream primer included the last codon of the *siaR* ORF, excluding the stop codon, to allow for the fusion of a multiple-histidine tag. The PCR product was cloned into pGEM-T and subsequently subcloned into pET-24(+) (Novagen, Madison, WI) using the HindIII and XhoI sites. The resulting plasmid, pJJ185, was expected to express SiaR with a carboxy-terminal His-tag.

Protein expression was induced using the Overnight Express Autoinduction System 1 (Novagen) grown at 20°C for 48 h. Expressed protein was purified using the BD TALON Metal Affinity Resin (BD Biosciences, Palo Alto, CA). Purification was performed in native conditions as follows. Cells from a 100 ml of expression culture were pelleted, re-suspended in 20 ml of equilibration buffer (300 mM NaCl, 50 mM sodium phosphate, pH 7.0) containing 2.5 $\mu\text{g ml}^{-1}$ DNase I (Sigma) and lysed with a French press. Cell debris was removed by ultracentrifugation at 150 000 g for 1 h. The BD TALON resin was prepared following the manufacturer's protocol and the lysate was loaded and allowed to bind for 1 h at room temperature. The resin was washed three times with 10 volumes of a high-salt wash buffer (1150 mM NaCl, 5 mM imidazole, 50 mM sodium phosphate, pH 7.0). Bound protein was eluted by washing three times with two volumes of elution buffer (300 mM NaCl, 500 mM imidazole, 50 mM sodium phosphate, pH 7.0). Eluted fractions were examined by SDS-PAGE and fractions containing SiaR were pooled and dialysed into a buffer that prevents the precipitation of purified protein (10 mM Tris, pH 8.0, 150 mM KCl, 1 mM DTT,

1 mM EDTA, 5 mM MgCl₂, 10% glycerol, 0.1% CHAPS). Aliquots of the purified protein were frozen in liquid nitrogen and stored at -80°C until needed. The protein was unstable and precipitated after purification, precluding the determination of a dissociation constant for the binding reaction.

Electrophoretic mobility shift assay

Electrophoretic mobility shift assay was used to study the binding of purified SiaR to potential promoter sequences. Probes for EMSA were amplified by PCR using primer pairs P146F1 and P146R3 (*siaP-nanE* intergenic region), licAUF1 and licAL3 (*lic1* promoter region) and P2F1 and P2R1 (P2 promoter). Binding reactions were prepared using the EMSA Kit (Molecular Probes, Eugene, OR) following the manufacturer's directions with some modifications. Pilot experiments were performed to determine the amount of SiaR required to shift all of the DNA probe. Binding reactions consisted of the binding buffer (150 mM KCl, 0.1 mM DTT, 0.1 mM EDTA, 10 mM Tris, pH 7.4), the DNA probe (15 nM) and 1 μM SiaR. Control reactions without SiaR were set up for each probe. Reactions were incubated at room temperature for 20 min. After incubation, 6 \times EMSA gel-loading solution was added and reactions were loaded onto a 6% DNA Retardation Gel (Invitrogen) with pre-chilled 0.5 \times TBE buffer and run at 200 V for 60 min. After electrophoresis, the gel was stained with SYBR Green EMSA gel stain and bands were visualized by UV transillumination. Images were captured using a Kodak EDAS 120 camera with an EDAS 590 mm filter (Eastman Kodak Company, Rochester, NY). To test the ability of various sugars to prevent SiaR binding, reactions were set up with the addition of 1 mM Neu5Ac, *N*-acetylmannosamine, *N*-acetylglucosamine or *N*-acetylglucosamine-6-phosphate.

DNase I footprint analysis

DNase I footprinting analysis of the *nanE-siaP* intergenic region was examined using the procedure of Johnson *et al.* (1979), with some modifications. The probe was prepared by PCR amplification with primers P146F1 and P146R4, resulting in a 257 bp fragment. The PCR product was cleaned up using the QIAquick PCR Purification Kit (Qiagen) and then digested with ApoI. The digested fragment was electrophoresed and a 209 bp fragment was purified using the MinElute Gel Extraction Kit (Qiagen). The purified fragment was end-labelled with [α -³²P]-dATP (GE Healthcare Bio-Sciences, Piscataway, NJ) and Klenow Fragment (3'-5' exo-; New England Biolabs). Probe was cleaned up using the MinElute Reaction Cleanup Kit (Qiagen). Approximately 100 ng of probe (800 000 cpm) were used per reaction.

DNase I footprinting reactions were set up in binding buffer (10 mM Tris, pH 8.0, 150 mM NaCl, 0.1 mM DTT, 1 mM EDTA, 10% glycerol and 0.1% CHAPS) containing 25 ng μl^{-1} salmon sperm DNA (Sigma), 1 μg μl^{-1} BSA (Sigma) and 100 ng of the probe. Purified SiaR was added to the reaction (90 μl total volume) at concentrations ranging from 0 to 2.5 μM and reactions were incubated at room temperature for 20 min to allow for DNA binding. DNase I (Sigma; 50 ng per reaction) and 10 \times digestion buffer (400 mM Tris, pH 7.5, 150 mM MgCl₂ and 50 mM CaCl₂) were added and reactions

were incubated at room temperature for 1 min prior to the addition of 100 μ l of stop solution (60 mM Tris, pH 8.0, 100 mM EDTA). Reaction was extracted with an equal volume of phenol-chloroform and DNA was precipitated with sodium acetate and ethanol with 5 μ g of glycogen (Sigma) added as a carrier. Dried DNA was re-suspended in 5 μ l of water and 2 \times formamide loading dye (98% deionized formamide, 10 mM EDTA, 0.025% xylene cyanol FF, 0.025% bromophenol blue) was added. Reactions were loaded onto an 8% sequencing gel with a G+A sequencing ladder made from the same probe. After electrophoresis, the gel was dried and exposed to film at -70°C .

Serum killing assay

NTHi strains 2019, JWJ070 and JWJ071 were grown to early log phase, OD_{600} of 0.2, in sBHI broth with and without 100 μM Neu5Ac. Bacteria were diluted to 1×10^7 cells per ml with phosphate-buffered salt solution (PBSS) consisting of 10 mM K_2HPO_4 , 10 mM KH_2PO_4 , 136 mM NaCl, 5 mM KCl, 1 mM CaCl_2 , 0.3 mM $\text{MgCl}_2 \cdot 6\text{H}_2\text{O}$, 1 mM $\text{MgSO}_4 \cdot 7\text{H}_2\text{O}$ and 0.01% BSA, pH 7.0.

The serum killing assay, modified from that reported by Andreoni *et al.* (1993), was carried out in a 96-well plate with a 200 μ l final volume. Pooled normal human serum (PNHS), a 20-donor pool of serum from human volunteers with no previous history of serious infections, was diluted to 10% in PBSS. A control containing PNHS that had been heat-inactivated for 30 min at 56°C was included in each experiment. Ten microlitres (1×10^5 organisms) of the re-suspended bacteria were diluted into 190 μ l of PBSS and serial 10-fold dilutions made in PBSS. Twenty microlitres of each dilution was spread on sBHI with or without appropriate antibiotic selection and grown overnight at 37°C in 5% CO_2 . Colonies were counted and used as the initial colony-forming units (cfu). Ten microlitres of the bacterial stock was incubated in the diluted serum at 37°C for 30 min with shaking at 200 r.p.m. Serial 10-fold dilutions of the reaction mixtures in PBSS were plated on sBHI with or without appropriate antibiotic selection. The plates were grown overnight at 37°C in 5% CO_2 and emerging colonies counted the next day. The resulting cfu value was that recorded after 30 min. Killing was assessed by comparing the number of cfu from the 30 min serum incubation with the number of the initial cfu. Results were expressed as the \log_{10} change in cfu at 30 min compared with the initial cfu. Statistical analysis of the data from bactericidal assays was carried out using the paired *t*-test and analysis of variance functions found in Graphpad Prism, version 4, San Diego, CA.

LOS preparation and neuraminidase treatment

Strains 2019*nanA*, 2019*siaP*, JWJ070 and JWJ071 were grown in sBHI containing 100 μM Neu5Ac. Five hundred millilitres of cultures were started with an OD_{600} of 0.05 and grown to an OD_{600} of 0.5 prior to harvesting the cells by centrifugation. Cell pellets were washed twice with PBS and then extracted with 25 ml of water-saturated phenol after both were equilibrated to 65°C . This mixture was cooled on ice for 1 h and separated by low-speed centrifugation. The top

aqueous layer was removed and saved. The phenol layer was back extracted once with water at 65°C , cooled, centrifuged, and the second aqueous layer added to the first. The residual phenol was removed from the LOS by precipitating the LOS twice using 0.3 M sodium acetate (final concentration) and two volumes of 100% ethanol. This was incubated at -20°C overnight and then centrifuged at 15 000 *g* for 30 min. To remove any contaminating lipoproteins, the LOS pellets were re-suspended in 8 ml of buffer A (60 mM Tris, 10 mM EDTA, 2.0% SDS, pH 6.8), and incubated in a boiling water bath for 5–10 min. The samples were allowed to cool, and proteinase K (Sigma) was added to a final concentration of 12.5 $\mu\text{g ml}^{-1}$. The samples were incubated at 37°C for 16–24 h. The LOS was precipitated as described above. The LOS was washed three times by precipitation, as above, with ethanol to remove any residual SDS. After the last precipitation, the LOS was washed twice with water and centrifugation at 100 000 *g* for 75 min. The pellets were re-suspended in water, frozen and then lyophilized. The dry LOS was stored at room temperature.

Quantification of total surface sialic acid

The TBA method of Warren (1959) was used to quantitatively compare the levels of sialic acid from purified LOS. Purified LOS was dissolved in a 100 mM sodium acetate, pH 5.6, buffer containing 0.05 U neuraminidase (Roche Applied Science), and incubated at 37°C overnight. At the end of the incubation the samples were centrifuged at 20 000 *g* to remove any precipitant and the supernatant was recovered for sialic acid analysis using the TBA method. Measurements were performed on three separate occasions with a standard curve performed with each set of samples.

Preparation of O-LOS

To make the LOS more amenable for mass spectrometric analysis, O-linked fatty acids were removed from the lipid A moiety as previously described (Gibson *et al.*, 1997). The highly purified LOS (~ 0.1 mg) was incubated in anhydrous hydrazine (50 μ l; Aldrich) at 37°C for 35 min with mixing every 10 min. Samples were cooled on ice prior to and after the addition of ice-cold acetone (250 μ l; Aldrich), then transferred to -20°C for 2 h. The quenched reaction mixture was centrifuged (12 000 *g*) for 45 min at 4°C . The supernatant was removed and the pelleted O-LOS was dissolved in MilliQ H_2O (50 μ l) and evaporated on a speed vacuum system (Savant). To remove salts and other low-molecular-weight contaminants the O-LOS (~ 20 – 30 μg) was suspended on a nitrocellulose membrane (type VS, 0.025 μm ; Millipore) over water for approximately 1 h. The desalted O-LOS was removed from the membrane concentrated with a speed vacuum system, and analysed by MALDI-LIT-MS.

Mass spectrometry of O-LOS

Aliquots of O-LOS were desalted by mixing with Dowex 50 beads (100–200 mesh, NH_4^+ form; Bio-Rad, Hercules, CA) prior to mass spectrometry. Mass spectrometric data were collected on a FinniganTM LTQTM linear ion trap-mass (LIT) spectrometer coupled to a vMALDI ion source (Thermo-

Electron, San Jose, CA). The vMALDI ion source operates at 170mTorr and uses an SI nitrogen laser (337.7 nm). Aliquots of the O-LOS (0.5 µl) were spotted onto a 96-well sample plate and allowed to dry. Dried samples were overlaid with 0.5 ml of 50 mg ml⁻¹ 2, 5 dihydroxybenzoic acid (DHB) in 50% acetonitrile. Data were collected in negative mode over two mass ranges: *m/z* 800–4000 and *m/z* 2000–4000. MS2 data were collected in negative mode to confirm sialylation, using a precursor isolation width of 3 *m/z*, normalized collision energy of 40% (RF amplitude in per cent used for fragment ions), activation Q of 0.25 and an activation time of 30 ms. Spectra were recorded using automatic gain control (AGC) to control the number of laser shots and the automatic spectrum filter (ASF) tool.

Acknowledgements

This work was supported by funding from NIAID Grants AI24616 and AI30040.

References

- Allen, S., Zaleski, A., Johnston, J.W., Gibson, B.W., and Apicella, M.A. (2005) Novel sialic acid transporter of *Haemophilus influenzae*. *Infect Immun* **73**: 5291–5300.
- Andreoni, J., Kayhty, H., and Densen, P. (1993) Vaccination and the role of capsular polysaccharide antibody in prevention of recurrent meningococcal disease in late complement component-deficient individuals. *J Infect Dis* **168**: 227–231.
- Bateman, A. (1999) The SIS domain: a phosphosugar-binding domain. *Trends Biochem Sci* **24**: 94–95.
- Bouchet, V., Hood, D.W., Li, J., Brisson, J.R., Randle, G.A., Martin, A., et al. (2003) Host-derived sialic acid is incorporated into *Haemophilus influenzae* lipopolysaccharide and is a major virulence factor in experimental otitis media. *Proc Natl Acad Sci USA* **100**: 8898–8903.
- Campagnari, A.A., Gupta, M.R., Dudas, K.C., Murphy, T.F., and Apicella, M.A. (1987) Antigenic diversity of lipooligosaccharides of nontypable *Haemophilus influenzae*. *Infect Immun* **55**: 882–887.
- Figueira, M.A., Ram, S., Goldstein, R., Hood, D.W., Moxon, E.R., and Pelton, S.I. (2007) Role of complement in defense of the middle ear revealed by restoring the virulence of nontypable *Haemophilus influenzae* *siaB* mutants. *Infect Immun* **75**: 325–333.
- Gibson, B.W., Engstrom, J.J., John, C.M., Hines, W., and Falick, A.M. (1997) Characterization of bacterial lipooligosaccharides by delayed extraction matrix-assisted laser desorption time-of-flight mass spectrometry. *J Am Soc Mass Spectrom* **8**: 645–658.
- Greiner, L.L., Watanabe, H., Phillips, N.J., Shao, J., Morgan, A., Zaleski, A., et al. (2004) Nontypable *Haemophilus influenzae* strain 2019 produces a biofilm containing *N*-acetylneuraminic acid that may mimic sialylated O-linked glycans. *Infect Immun* **72**: 4249–4260.
- Harrison, A., Ray, W.C., Baker, B.D., Armbruster, D.W., Bakaletz, L.O., and Munson, R.S., Jr (2007) The OxyR regulon in nontypable *Haemophilus influenzae*. *J Bacteriol* **189**: 1004–1012.
- Hegde, P., Qi, R., Abernathy, K., Gay, C., Dharap, S., Gaspard, R., et al. (2000) A concise guide to cDNA microarray analysis. *Biotechniques* **29**: 548–550, 552–544, 556 passim.
- Herriott, R.M., Meyer, E.M., and Vogt, M. (1970) Defined nongrowth media for stage II development of competence in *Haemophilus influenzae*. *J Bacteriol* **101**: 517–524.
- Hood, D.W., Makepeace, K., Deadman, M.E., Rest, R.F., Thibault, P., Martin, A., et al. (1999) Sialic acid in the lipopolysaccharide of *Haemophilus influenzae*: strain distribution, influence on serum resistance and structural characterization. *Mol Microbiol* **33**: 679–692.
- Hood, D.W., Cox, A.D., Gilbert, M., Makepeace, K., Walsh, S., Deadman, M.E., et al. (2001) Identification of a lipopolysaccharide alpha-2,3-sialyltransferase from *Haemophilus influenzae*. *Mol Microbiol* **39**: 341–350.
- Johnson, A.D., Meyer, B.J., and Ptashne, M. (1979) Interactions between DNA-bound repressors govern regulation by the lambda phage repressor. *PNAS* **76**: 5061–5065.
- Jurcisek, J., Greiner, L., Watanabe, H., Zaleski, A., Apicella, M.A., and Bakaletz, L.O. (2005) Role of sialic acid and complex carbohydrate biosynthesis in biofilm formation by nontypable *Haemophilus influenzae* in the chinchilla middle ear. *Infect Immun* **73**: 3210–3218.
- Kalivoda, K.A., Steenbergen, S.M., Vimr, E.R., and Plumbridge, J. (2003) Regulation of sialic acid catabolism by the DNA binding protein NanR in *Escherichia coli*. *J Bacteriol* **185**: 4806–4815.
- Mandrell, R.E., McLaughlin, R., Aba Kwaik, Y., Lesse, A., Yamasaki, R., Gibson, B., et al. (1992) Lipooligosaccharides (LOS) of some *Haemophilus* species mimic human glycosphingolipids, and some LOS are sialylated. *Infect Immun* **60**: 1322–1328.
- Menard, R., Sansonetti, P.J., and Parsot, C. (1993) Nonpolar mutagenesis of the *ipa* genes defines IpaB, IpaC, and IpaD as effectors of *Shigella flexneri* entry into epithelial cells. *J Bacteriol* **175**: 5899–5906.
- Munson, R., Jr, and Tolan, R.W., Jr (1989) Molecular cloning, expression, and primary sequence of outer membrane protein P2 of *Haemophilus influenzae* type b. *Infect Immun* **57**: 88–94.
- Peterson, S., Cline, R.T., Tettelin, H., Sharov, V., and Morrison, D.A. (2000) Gene expression analysis of the *Streptococcus pneumoniae* competence regulons by use of DNA microarrays. *J Bacteriol* **182**: 6192–6202.
- Plumbridge, J., and Vimr, E. (1999) Convergent pathways for utilization of the amino sugars *N*-acetylglucosamine, *N*-acetylmannosamine, and *N*-acetylneuraminic acid by *Escherichia coli*. *J Bacteriol* **181**: 47–54.
- Redfield, R.J., Cameron, A.D., Qian, Q., Hinds, J., Ali, T.R., Kroll, J.S., and Langford, P.R. (2005) A novel CRP-dependent regulon controls expression of competence genes in *Haemophilus influenzae*. *J Mol Biol* **347**: 735–747.
- Ringenberg, M.A., Steenbergen, S.M., and Vimr, E.R. (2003) The first committed step in the biosynthesis of sialic acid by *Escherichia coli* K1 does not involve a phosphorylated *N*-acetylmannosamine intermediate. *Mol Microbiol* **50**: 961–975.
- Severi, E., Randle, G., Kivlin, P., Whitfield, K., Young, R., Moxon, R., et al. (2005) Sialic acid transport in *Haemophi-*

- lus influenzae* is essential for lipopolysaccharide sialylation and serum resistance and is dependent on a novel tripartite ATP-independent periplasmic transporter. *Mol Microbiol* **58**: 1173–1185.
- Sorensen, K.I., and Hove-Jensen, B. (1996) Ribose catabolism of *Escherichia coli*: characterization of the *rpiB* gene encoding ribose phosphate isomerase B and of the *rpiR* gene, which is involved in regulation of *rpiB* expression. *J Bacteriol* **178**: 1003–1011.
- Vimr, E.R., and Troy, F.A. (1985) Identification of an inducible catabolic system for sialic acids (*nan*) in *Escherichia coli*. *J Bacteriol* **164**: 845–853.
- Vimr, E., Steenbergen, S., and Cieslewicz, M. (1995) Biosynthesis of the polysialic acid capsule in *Escherichia coli* K1. *J Ind Microbiol* **15**: 352–360.
- Vimr, E., Lichtensteiger, C., and Steenbergen, S. (2000) Sialic acid metabolism's dual function in *Haemophilus influenzae*. *Mol Microbiol* **36**: 1113–1123.
- Vimr, E.R., Kalivoda, K.A., Deszo, E.L., and Steenbergen, S.M. (2004) Diversity of microbial sialic acid metabolism. *Microbiol Mol Biol Rev* **68**: 132–153.
- Warren, L. (1959) The thiobarbituric acid assay of sialic acids. *J Biol Chem* **234**: 1971–1975.
- Weiser, J.N., Maskell, D.J., Butler, P.D., Lindberg, A.A., and Moxon, E.R. (1990) Characterization of repetitive sequences controlling phase variation of *Haemophilus influenzae* lipopolysaccharide. *J Bacteriol* **172**: 3304–3309.
- Weiser, J.N., Pan, N., McGowan, K.L., Musher, D., Martin, A., and Richards, J. (1998) Phosphorylcholine on the lipopolysaccharide of *Haemophilus influenzae* contributes to persistence in the respiratory tract and sensitivity to serum killing mediated by C-reactive protein. *J Exp Med* **187**: 631–640.
- Whitby, P.W., Morton, D.J., and Stull, T.L. (1998) Construction of antibiotic resistance cassettes with multiple paired restriction sites for insertional mutagenesis of *Haemophilus influenzae*. *FEMS Microbiol Lett* **158**: 57–60.

Supplementary material

The following supplementary material is available for this article:

This material is available as part of the online article from:
<http://www.blackwell-synergy.com/doi/abs/10.1111/j.1365-2958.2007.05890.x>

(This link will take you to the article abstract).

Please note: Blackwell Publishing is not responsible for the content or functionality of any supplementary materials supplied by the authors. Any queries (other than missing material) should be directed to the corresponding author for the article.